Original research

The immunologic phenotype of thrombi is associated with future vascular events after cerebral infarction

Wookjin Yang ![ORCID],[1] Soon Auck Hong,[2] Jeong-Min Kim ![ORCID],[1] Hae-Bong Jeong ![ORCID],[3] Taek-Kyun Nam,[4] Hyun Ho Choi ![ORCID],[4] Suh Min Kim,[5] Kwang-Yeol Park,[3] Hye Ryoun Kim[6]

ABSTRACT

Background Thrombi retrieved from patients with acute ischemic stroke may contain prognostic information.
Objective To investigate the relationship between the immunologic phenotype of thrombi and future vascular events in patients with a stroke.
Methods This study included patients with acute ischemic stroke who underwent endovascular thrombectomy at Chung-Ang University Hospital in Seoul, Korea, between February 2017 and January 2020. Laboratory and histological variables were compared between patients with and without recurrent vascular events (RVEs). Kaplan–Meier analysis followed by the Cox proportional hazards model was used to identify factors related to RVE. Receiver operating characteristic (ROC) analysis was conducted to evaluate the performance of the immunologic score by combining immunohistochemical phenotypes to predict RVE.
Results A total of 46 patients were included in the study with 13 RVEs (mean±SD age, 72.8±11.3 years; 26 (56.5%) men). Thrombi with a lower percentage of programmed death ligand-1 expression (HR=11.64; 95% CI 1.60 to 84.82) and a higher number of citrullinated histone H3 positive cells (HR=4.19; 95% CI 0.81 to 21.75) were associated with RVE. The presence of high-mobility group box 1 positive cell was associated with reduced risk of RVE, but the association was lost after adjustment for stroke severity. The immunologic score, which consists of the three immunohistochemical phenotypes, showed good performance in predicting RVE (area under the ROC curve, 0.858; 95% CI 0.758 to 0.958).
Conclusions The immunological phenotype of thrombi could provide prognostic information after stroke.

WHAT IS ALREADY KNOWN ON THIS TOPIC

⇒ Conventional histological examinations of thrombi retrieved by endovascular thrombectomy offer clues to distinguish stroke etiology. Recent studies have demonstrated that the immunologic features of thrombi might also be associated with clinical outcomes, such as early neurological deterioration, in patients with acute ischemic stroke.

WHAT THIS STUDY ADDS

⇒ In this study, the immunologic features of endovascular thrombectomy-retrieved thrombi including programmed death ligand-1 proportion, negative high mobility group box 1, and high citrullinated histone H3 expression were linked to a higher risk of future vascular events in patients with acute ischemic stroke.

HOW THIS STUDY MIGHT AFFECT RESEARCH, PRACTICE OR POLICY

⇒ Endovascular thrombectomy-retrieved thrombi may provide prognostic clue after ischemic stroke. The immunologic features of thrombi may merit additional investigation as potential therapeutic targets for reducing recurrent vascular events.

INTRODUCTION

Endovascular thrombectomy (EVT) has significantly improved the treatment outcome of acute ischemic stroke (AIS) with large-vessel occlusion; however, stroke survivors are known to experience various recurrent vascular events (RVEs). Despite optimal secondary prevention therapy, approximately 20–30% of patients with a stroke who undergo EVT reportedly experience a RVE 5 years after the procedure.[1 2]

Conventional histological analyses of retrieved thrombi have focused on clot composition, such as red blood cells, platelets, and fibrin, which may help to determine stroke etiology.[3–6] Furthermore, several studies have suggested that the immunologic profile of thrombi can have prognostic implications. The content of neutrophil extracellular traps (NETs) in thrombi has recently emerged as a promising marker to predict neurological outcome after stroke because it is associated with resistance to thrombolytic therapy.[6–9] Several damage-associated molecular pattern molecules have been proved to induce NETosis and thrombosis, with high-mobility group box 1 (HMGB1) playing a critical role.[10] In addition, our recent study analyzed the microRNA expression pattern of the thrombus and found that elevated miR-93–5 p, which may inhibit the immune checkpoint protein programmed death ligand-1 (PD-L1),[11] was associated with an increased risk of early neurological deterioration after index stroke.[12]

Given this prognostic potential of immunologic profile of retrieved thrombus, we aimed to assess the association between immunologic phenotypes of thrombi and RVEs and establish thrombus-based

prognostic tools for patients with stroke who underwent EVT in the present study.

METHODS

Study population

The Thrombus Analysis of Ischemic Stroke, single-center prospective registry for patients with AIS who have received EVT at Chung-Ang University Hospital, aimed to broaden the understanding of stroke based on thrombus analysis. We reviewed consecutive patients between February 2017 and January 2020, and those whose thrombi were not suitable for histological and immunohistochemical analyses were excluded. The institutional review board of the Chung-Ang University Hospital approved this study (IRB number: 1621-003-264). Informed consent was obtained from patients or their caregivers/guardians.

Data collection

Information on age, sex, hypertension, diabetes, hyperlipidemia, stroke history, smoking status, coronary artery disease, atrial fibrillation (AF), initial National Institutes of Health Stroke Scale (NIHSS) score, and discharge modified Rankin Scale score were obtained. The Trial of ORG 10172 in Acute Stroke Treatment classification for each patient was assessed with minor modifications, which further classified cardioembolic stroke into cardioembolism due to AF (CEA) and cardioembolism due to valvular heart disease or wall motion abnormalities, with or without AF (CEV). Occlusion site was assessed based on the initial angiography. Clot weight was measured in a subset of patients, specifically those included since March 2019. Laboratory findings, including complete blood count, estimated glomerular filtration rate, low-density lipoprotein cholesterol, triglyceride, glucose, and high-sensitivity C-reactive protein, were collected during admission. Left ventricular ejection fraction and left atrial size were assessed using routine echocardiography. Based on our previous report indicating a close relationship between bone metabolism and the risk of a future vascular event after a stroke,[13] bone mineralization status was measured by dual energy X-ray absorptiometry (Lunar Prodigy; GE Medical System, Madison, Wisconsin, USA) at the lumbar spine (first to fourth) and total hip joints following standardized procedures recommended by the International Society for Clinical Densitometry for the diagnosis of osteoporosis in clinical practice.[14] RVE was defined as the occurrence of objectively proven thromboembolic events or vascular deaths since the day of EVT and was used as the clinical outcome.

Tissue processing

The thrombus retrieved from EVT was promptly stored in a nitrogen tank at a temperature below −70°C. The retrieved thrombi were subjected to a histological examination when a sufficient number of thrombi were registered. Each thrombus was divided into two halves, with one half dissolved to extract microRNAs and the other half used for histological analysis. Since the primary objective of thrombus collection was to investigate stroke mechanism based on the microRNA expression signatures, the entire thrombus was used for RNA content analysis when the size of the thrombus was relatively small.[12] The pieces of thrombi for histological evaluation were embedded in paraffin after being fixed in 10% neutral buffered formalin. Thereafter, the specimens were sliced into 4 μm sections. The processed thrombi were analyzed using hematoxylin and eosin staining, followed by immunohistochemical analysis. Any remaining thrombi underwent multiplex tissue microarray immunohistochemical analysis (online supplemental figure S1).

Histopathological analysis

Hematoxylin and eosin staining was performed using the Leica ST5010 Autostainer XL (Leica, Wetzlar, Germany). A board-certified pathologist (SAH) blinded to the clinical information assessed the white blood cell and red blood cell components. Two to five distinct locations of each thrombus were examined depending on its size and heterogeneity, and the intensity of white blood cell infiltration was categorized into three grades: grade 1, <10 cells in ×400 fields; grade 2, 10–100 cells; and grade 3, >100. The relative proportion of red blood cells was rated as follows: grade 1, <30% of the sectioned area; grade 2, 30–70%; and grade 3, >70%.

Immunohistochemical staining was conducted using the Ventana Benchmark Autostainer (Ventana Medical Systems, Tucson, Arizona, USA). The sections of the retrieved thrombi were incubated with the following primary antibodies: myeloperoxidase (MPO) (A0398, Dako, Glostrup, Denmark; to identify neutrophils), CD41 (ab134131, Abcam, Cambridge, UK; to identify platelets), CD68 (M0876, Dako, Glostrup, Denmark; to identify macrophages), glycosphorin A (ab129024, Abcam, Cambridge, UK; to identify red blood cells), fibrinogen (ab34269, Abcam, Cambridge, UK), PD-L1 (M3653, Dako, Glostrup, Denmark), programmed death ligand-1 (PD-L2) (TA806581, OriGene, Rockville, Maryland, USA), HMGB1 (NB100-2322, Novus Biologicals, Centennial, Colorado, USA), and citrullinated histone H3 (H3Cit) (ab5103, Abcam, Cambridge, UK). An ultraview polymer detection kit (Ventana Medical System, Tucson, Arizona, USA) was used for visualization. Non-immune normal immunoglobulin G was used as a negative control to replace the primary antibodies, and no staining occurred.

Differential quantification was used to assess nucleated cells, anucleate cells, and subcellular proteins. For the nucleated cells, the board-certified pathologist (SAH) determined three hot spot areas based on the high number of nucleated cells and their cell viability, and the average numbers of stained cells for MPO, CD68, PD-L2, HMGB1, and H3Cit were calculated at ×400 magnification. The expression of anucleate cells and subcellular proteins, including CD41, glycosphorin A, fibrinogen, and PD-L1, was evaluated based on the proportion of staining, represented as the percentage of the stained area from the total thrombus area.

Multiplex immunohistochemistry

Multiplex immunohistochemical staining with tissue microarray was conducted to outline the distribution and co-localization of the immune cell markers in EVT-retrieved thrombus; the implementation and analysis was done in SuperBioChips Laboratories (Seoul, Korea).[15] In brief, 4 μm thick sections from tissue microarray were deparaffinized in xylene and dehydrated in graded ethanol. For nuclear staining, slides were incubated with Harris hematoxylin (Merck, Darmstadt, Germany) and washed with tap water and 1% hydrogen chloride solution. Tris-ethylenediaminetetraacetic acid buffer (pH 9.0), citrate buffer (pH 6.0), and the microwaves were used for antigen retrieval. We constructed two independent tissue microarray panels after considering the primary immunohistochemical staining results showing that PD-L1 expression was co-localized with CD41 expression, a marker of platelets.

The first panel consisted of PD-L1, CD41 and glycosphorin A and focused on the distribution pattern of PD-L1 and its interaction with platelets and red blood cells. The second panel

consisted of HMGB1, H3Cit, PD-L2, and MPO, focusing on interactions among nucleated immune cells and their distribution patterns. The sections were incubated with primary antibodies and washed twice with wash buffer (Dako, Carpinteria, California, USA), followed by Envision FLEX+mouse linker/rabbit linker (Dako, Carpinteria, California, USA) as a secondary reagent. ImmPact NovaRED (Vector Laboratories, Burlingame, California, USA) was used to detect and visualize chromogenic reactions. Nuclear counterstaining was performed using Mayer's hematoxylin. The stained slides were scanned using Aperio AT2 (Leica Biosystems, Newcastle on Tyne, UK), treated with stripping buffer, and microwaved to remove the antibody complex. The staining cycles were repeated for each antibody. Images were processed to adjust the cropped core image alignment and were analyzed using CellProfiler (version 3.1.8 Broad Institute, Cambridge, Massachusetts, USA). The cut-off values for each marker were designated from either manual inspection of immunostained images or from analysis of the distribution of staining intensity to find reasonable cut-off values.[15]

Statistical methods

Continuous variables are expressed as mean±SD or median (IQR) and compared using Student's t-test or Mann–Whitney U test, as appropriate. Categorical variables are expressed as the number of patients (percentage) and compared using the X^2 test or Fisher's exact test, as appropriate. X-tile software (version 3.6.1, Yale University, Connecticut, USA) was used to determine optimal cut-off values of immunohistochemical markers including PD-L1, HMGB1, and H3Cit to predict RVE, based on the highest X^2 values and the lowest P values.[16] PD-L1, HMGB1, and H3Cit were then converted into dichotomous variables using their optimal cut-off values. Based on all the possible combinations of the three immunohistochemical markers, four immunological scores were defined as the sum of 0 or 1 for each dichotomous variable. Cumulative incidence curves were plotted using Kaplan–Meier methods with log-rank tests to estimate cumulative incidence rates of RVE using the dichotomous PD-L1, HMGB1, H3Cit, and immunologic score combining all the immunohistochemical markers. The Cox proportional hazards model was used to evaluate the hazard ratios of RVE depending on each immunohistochemical marker and immunologic score, adjusting for age, sex, and variables with P<0.05 in bivariate analysis. The area under the receiver operating characteristic curves was calculated to assess the performance to predict RVE by the immunologic scores. To understand the mechanistic implication of the immunologic phenotype in thrombus formation, Spearman correlation analysis was performed between the immunologic phenotype and laboratory findings. Two-sided probability values with P<0.05 were considered statistically significant. Statistical analyses were performed using R (version 4.1.3, R Foundation, Vienna, Austria).

RESULTS

Among the 91 thrombi retrieved during the study period, a total of 46 cases were eligible for the final analysis (mean±SD of age, 72.8±11.3 years; 26 (56.5%) men) after excluding 45 inadequate specimens (online supplemental figure S1). Thirteen out of 46 patients developed RVE during the mean±SD follow-up period of 16.8±19.8 months (online supplemental table S1). Patients who experienced RVE presented with more severe neurological deficits, and their neurological outcomes were less favorable than those in the no RVE group. Despite similarities in the demographic and clinical factors between the two groups, the RVE group showed a lower neutrophil/higher

Table 1 Baseline characteristics according to recurrent vascular event

Characteristics	No RVE (n=33)	RVE (n=13)	P value
Age, years	77 (61–82)	72 (63–82)	0.97
Male sex	18 (54.5%)	8 (61.5%)	0.92
Hypertension	18 (54.5%)	9 (69.2%)	0.56
Diabetes	7 (21.2%)	5 (38.5%)	0.28*
Stroke history	7 (21.2%)	3 (23.1%)	>0.99*
Smoking	6 (18.2%)	3 (23.1%)	0.70*
Coronary artery disease	3 (9.1%)	1 (7.7%)	>0.99*
Atrial fibrillation	20 (60.6%)	6 (46.2%)	0.58
Initial NIHSS score	15.0±6.4	20.7±5.5	0.007
Discharge mRS score	2.8±1.7	4.5±1.3	0.004
Stroke etiology			0.17*
LAA	2 (6.1%)	4 (30.8%)	
CEA	17 (51.5%)	4 (30.8%)	
CEV	10 (30.3%)	3 (23.1%)	
Others	4 (12.1%)	2 (15.4%)	
Occlusion site			0.13*
Extracranial ICA	2 (6.1%)	1 (7.7%)	
Intracranial ICA	3 (9.1%)	2 (15.4%)	
Middle cerebral artery	22 (66.7%)	4 (30.8%)	
Vertebral artery	1 (3.0%)	2 (15.4%)	
Basilar artery	5 (15.2%)	4 (30.8%)	
Clot weight, g†	58.4±32.6	81.5±47.8	0.25
White blood cells, ×10⁹/L	8450 (6220–10 950)	6350 (4720–8900)	0.051
Neutrophil, %	79.9 (54.0–86.8)	62.3 (47.6–68.5)	0.038
Lymphocyte, %	14.2 (7.5–36.5)	29.4 (24.0–38.2)	0.11
Monocyte, %	5.7 (4.6–7.2)	7.8 (6.6–9.6)	0.004
Hemoglobin, g/dL	12.6±2.3	13.5±2.1	0.22
Platelet, ×10⁹/L	210.3±59.9	203.0±63.1	0.72
eGFR, mL/min/1.73 m2	87.2±25.4	74.8±28.0	0.16
LDL cholesterol, mg/dL	95.3±25.7	92.4±34.1	0.75
Triglyceride, mg/dL	83 (61.5–103.5)	137 (70–161)	0.029
Glucose, mg/dL	123 (109–165)	128 (116–197)	0.35
hsCRP, mg/dL	1.5 (0.9–4.6)	1.6 (1.1–4.2)	0.65
Left ventricular ejection fraction, %	63 (55–66)	62 (59–66)	0.91
Left atrial size, mm	44.2±9.4	40.5±13.0	0.29
BMD T-score at lumbar spine	−0.7±2.1	−0.4±2.2	0.70
BMD T-score at total hip	−1.3±1.4	−1.2±1.2	0.89

Data are expressed as number (%), mean±SD, or median (IQR).
*Analyzed using Fisher's exact test.
†Data available for 22 patients, including 18 patients without RVE and 4 patients with RVE.
BMD, bone mineral density; CEA, cardioembolism due to atrial fibrillation; CEV, cardioembolism due to valvular heart disease or wall motion abnormalities, with or without atrial fibrillation; eGFR, estimated glomerular filtration rate; hsCRP, high-sensitivity C-reactive protein; ICA, internal carotid artery; LAA, large artery atherosclerosis; LDL, low-density lipoprotein; mRS, modified Rankin Scale; NIHSS, National Institutes of Health Stroke Scale; RVE, recurrent vascular event.;

monocyte proportion and higher triglyceride levels in venous blood compared to the no RVE group (table 1).

The composition of red or white blood cells from hematoxylin and eosin staining and the immunohistochemical markers of

Table 2 Correlation between histological/immunohistochemical findings and recurrent vascular event

	No RVE (n=33)	RVE (n=13)	P value
WBC grade			0.25*
Grade 1	1 (3.0%)	1 (7.7%)	
Grade 2	7 (21.2%)	5 (38.5%)	
Grade 3	25 (75.8%)	7 (53.8%)	
RBC grade			0.75*
Grade 1	7 (21.2%)	2 (15.4%)	
Grade 2	10 (30.3%)	3 (23.1%)	
Grade 3	16 (48.5%)	8 (61.5%)	
MPO, number of cells/x400 HPF	100.3±68.6	86.8±46.4	0.52
CD41, %	58±29	54±24	0.64
CD68, number of cells/x400 HPF	29.8±14.5	27.1±12.5	0.55
Glycosphorin A, %	72±22	78±18	0.36
Fibrinogen, %	68±24	72±23	0.58
PD-L1, %	36±24	19±18	0.027
PD-L2, number of cells/x400 HPF	13.2±10.1	9.5±6.4	0.23
HMGB1, number of cells/x400 HPF	11.9±14.7	2.8±5.7	0.004
H3Cit, number of cells/x400 HPF	14.5±18.2	28.0±27.8	0.059

Data are expressed as number (%) or mean±SD.
*Analyzed using Fisher's exact test.
H3Cit, citrullinated histone H3; HMGB1, high-mobility group box 1; HPF, high power field; MPO, myeloperoxidase; PD-L2, programmed death ligand-2; PD-L1, programmed death ligand-1; RBC, red blood cell; RVE, recurrent vascular event; WBC, white blood cell.

Figure 1 Representative thrombus characteristics of the patients with and without recurrent vascular event (A) H&E and immunohistochemical staining of thrombus retrieved from the left middle cerebral artery occlusion in a patient who had a stable prognosis during the follow-up period. (B) H&E and immunohistochemical staining of thrombus retrieved from the right middle cerebral artery occlusion in a patient who experienced another right middle cerebral artery infarction 10 months after the index stroke. Fib, fibrinogen; GSA, glycosphorin A; H&E, hematoxylin and eosin; H3Cit, citrullinated histone H3; HMGB1, high-mobility group box 1; MPO, myeloperoxidase; PD-L1, programmed death ligand-1; PD-L2, programmed death ligand-2.

conventional thrombus components, including red blood cells, white blood cells, platelets, and fibrinogen, were not significantly different between the two groups. However, the proportion of PD-L1 expression area and the number of HMGB1-positive cells were significantly lower in the thrombi from the RVE group than in the no RVE group. Thrombi retrieved from the RVE group tended to have a higher H3Cit-positive cell count than those retrieved from the no RVE group (table 2).

The representative image of the thrombus from the patient with stable prognosis (figure 1A) and that from the patient who experienced another stroke 10 months after the index stroke (figure 1B) showed several diverse immunological characteristics, such as a reduced proportion of PD-L1 staining area, absent HMGB1-positive cells, and increased expression of H3Cit in the thrombus, with detrimental outcomes. Another interesting finding is the correlation between PD-L1 and CD41 staining area within the thrombus, suggesting that platelets are a major determinant of PD-L1 expression in the thrombus. Multiplex tissue immunohistochemistry with three markers, including PD-L1 (green), glycosphorin A (red), and CD41 (blue), also showed that thrombi with stable prognosis were associated with a higher proportion of PD-L1-positive area than those from patients with RVEs. The sky-blue area represents the area of PD-L1 and CD41 co-expression, suggesting that platelets express PD-L1 (figure 2). Multiplex tissue immunohistochemistry targeting cells with HMGB1 (green), H3Cit (red), PD-L2 (blue), and MPO (red circle) showed that patients with stable prognosis had a higher number of HMGB1-positive cells than those from patients with RVEs (figure 3).

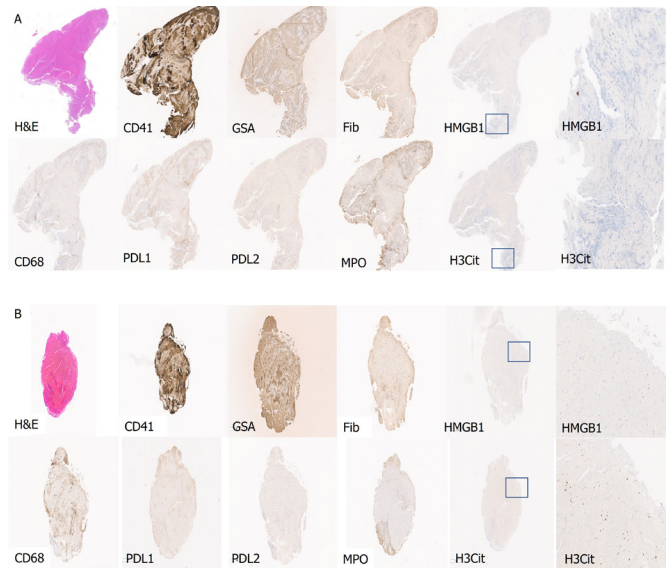The optimal cut-off values of the above three immunohistochemical markers for the association with RVE were as follows: PD-L1, <15% ($X^2=9.1431$; P=0.003); HMGB1, <1 ($X^2=3.9755$; P=0.046); and H3Cit, ≥18 ($X^2=5.5689$; P=0.018). The cumulative incidence of RVE was significantly higher in patients with thrombi with a lower PD-L1 proportion, negative HMGB1 expression, higher H3Cit expression, and higher immunologic score (figure 4). The Cox proportional hazards models showed similar results for PD-L1, H3Cit, and immunologic scores combining two or three markers. However, the correlations of HMGB1 and the immunologic score combining HMGB1 and H3Cit with RVE were lost after adjusting for covariates including initial NIHSS score and discharge modified Rankin Scale score (table 3). Among immunologic scores, the combination of all three immunohistochemical markers showed the best performance in predicting RVE (online supplemental figure S2 and online supplemental table S2).

The proportion of PD-L1 in thrombi correlated with the proportion of CD41 (Spearman's ρ, 0.73; p<0.001; online supplemental figure S3A), CD68-positive cell numbers (Spearman's ρ, 0.50; p<0.001; online supplemental figure S3B), and MPO-positive cell numbers (Spearman's ρ, 0.36; P=0.014; online supplemental figure S3C) in thrombi. The H3Cit-positive cells in the thrombus showed a tendency of correlation with CD68-positive cells (Spearman's ρ, 0.29; P=0.051; online supplemental figure S3D) and inversely correlated with the proportion of CD41 expression in thrombi (Spearman's ρ, −0.32, P=0.028; online supplemental figure S3E), but were not related to MPO-positive cells (Spearman's ρ, 0.099; P=0.50). The number of HMGB1-positive cells in thrombi was not associated with the proportion of PD-L1 (Spearman's ρ, 0.047; P=0.75; online supplemental figure S3F) or with the number of H3Cit-positive cells (Spearman's ρ, 0.014; P=0.93). Among
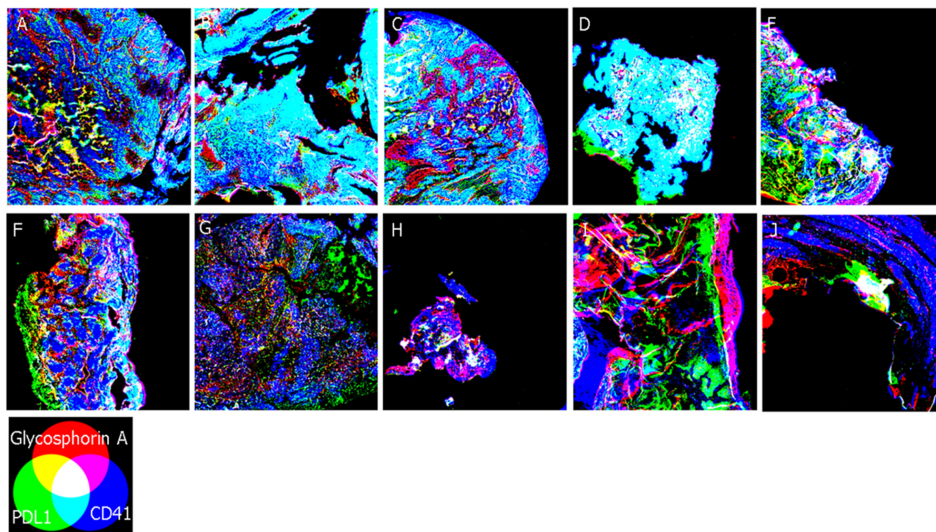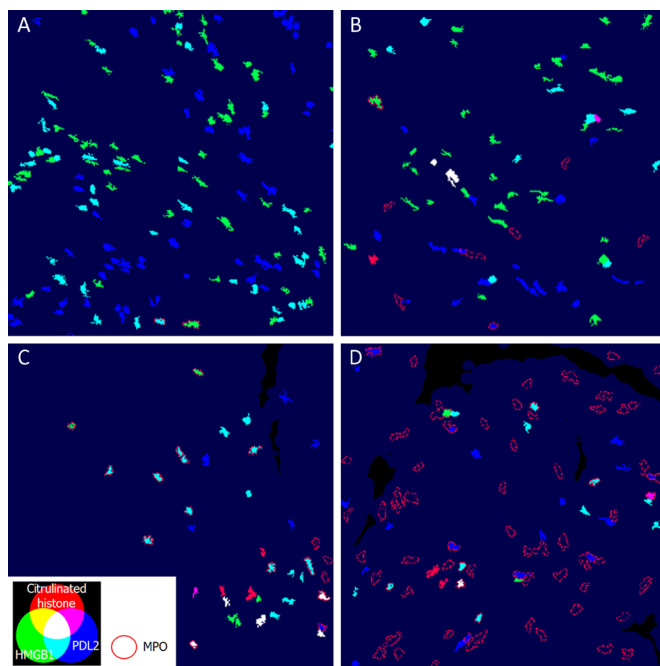
Figure 2 Representative images of multiplex tissue immunohistochemistry panel 1 from the thrombi with and without recurrent vascular events Pseudocolor-assigned images reconstructed from multiplex tissue immunohistochemistry panel 1, which illustrate the co-expression of PD-L1 and markers of platelets (CD41) and red blood cells (glycosphorin A) within thrombi retrieved from (A–E) patients with recurrent vascular events and (F–J) patients without recurrent vascular events. PD-L1, programmed death ligand-1. Magnification x40.

exploratory correlation analysis between histological profile and laboratory data, the number of HMGB1-positive cells in thrombi was associated with bone mineral density measured as a T-score at the spine (Spearman's ρ, 0.38; P=0.028).

Figure 3 Representative images of multiplex tissue immunohistochemistry panel 2 from the thrombi with and without recurrent vascular events Pseudocolor-assigned images reconstructed from multiplex tissue immunohistochemistry panel 2, which illustrate the co-expression of HMGB1, H3Cit, PD-L2, and a neutrophil marker (MPO) within thrombi retrieved from patients with stable prognosis (A–B) and with recurrent vascular events (C–D). H3Cit, citrullinated histone H3; HMGB1, high-mobility group box 1; MPO, myeloperoxidase; PD-L2, programmed death ligand-2. Magnification x400.

DISCUSSION

This study demonstrated that the immunologic phenotypes of thrombus, specifically lower PD-L1 proportion, negative HMGB1 expression, and higher H3Cit expression, were associated with RVE among stroke survivors. The immunologic scores of the three immunohistochemical markers presented their potential to predict RVE. The exaggerated innate immune response by increased NETosis and attenuated immune-modulating signal by decreased PD-L1 expression from the thrombus could be a warning sign of future vascular events among stroke survivors.
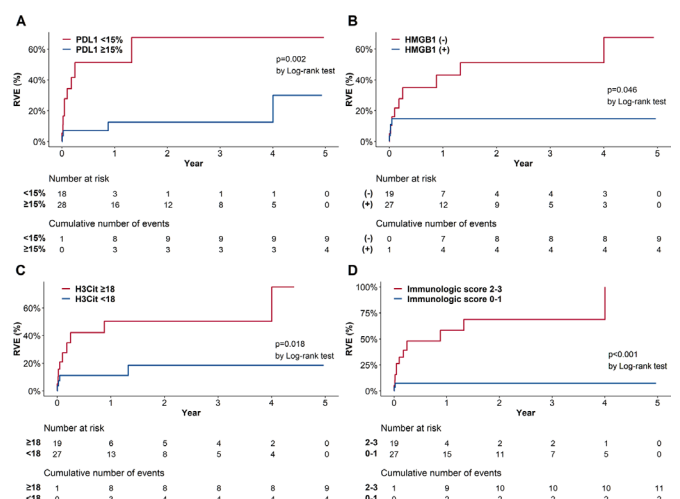

Figure 4 Cumulative incidence curves of recurrent vascular event according to dichotomous immunohistochemical markers and the immunologic score combining the three markers cumulative incidence of recurrent vascular events according to dichotomous (A) PD-L1, (B) HMGB1, (C) H3Cit, and (D) immunologic score combining all three immunohistochemical markers. Log-rank tests were performed to determine the statistical significance. abbreviations: H3Cit, citrullinated histone H3; HMGB1, high-mobility group box 1; PD-L1, programmed death ligand-1; RVE, recurrent vascular event.

Table 3 Hazard of recurrent vascular event according to the immunohistochemical markers and the immunologic scores

	Unadjusted HR (95% CI)	P value	Adjusted HR (95% CI)*	P value
PD-L1	0.65 (0.44 to 0.95)	0.027	0.63 (0.40 to 1.00)	0.0497
<15%	5.55 (1.66 to 18.61)	0.006	11.64 (1.60 to 84.82)	0.016
≥15%	Reference		Reference	
HMGB1	0.93 (0.85 to 1.01)	0.085	0.94 (0.84 to 1.05)	0.28
Negative	3.11 (0.96 to 10.13)	0.059	0.83 (0.14 to 4.96)	0.84
Positive	Reference		Reference	
H3Cit	1.02 (0.98 to 1.04)	0.089	1.03 (1.00 to 1.06)	0.059
<18	Reference		Reference	
≥18	3.78 (1.16 to 12.29)	0.027	4.19 (0.81 to 21.75)	0.088
Immunologic scores				
PD-L1+HMGB1	4.03 (1.68 to 9.67)	0.002	3.36 (0.98 to 11.53)	0.054
PD-L1+H3Cit	4.41 (1.85 to 10.52)	<0.001	3.45 (1.19 to 10.03)	0.023
HMGB1+H3Cit	3.26 (1.43 to 7.40)	0.005	2.01 (0.64 to 6.33)	0.23
PD-L1+HMGB1+H3Cit	4.08 (1.92 to 8.68)	<0.001	2.48 (1.04 to 5.93)	0.040

*Adjusted for age, sex, proportions of neutrophils and monocytes, triglyceride, initial NIHSS score, and functional independence at discharge (mRS score 0–2 or 3–6).
H3Cit, citrullinated histone H3; HMGB1, high-mobility group box 1; mRS, modified Rankin Scale; NIHSS, National Institutes of Health Stroke Scale; PD-L1, programmed death ligand-1.

We found that decreased expression of PD-L1 in the thrombus was related to RVE in patients with AIS and that PD-L1 is abundantly expressed in platelets. Programmed death protein-1 (PD-1)/PD-L1 are immune checkpoint inhibitors that have been actively investigated as therapeutic targets in the field of oncology,[17] and are reportedly involved in neurological disorders including stroke.[18] The PD-1/PD-L1 pathway has been suggested to be crucial in downregulating proatherogenic T-cells and proinflammatory cytokines in previous studies.[19 20] Inhibiting the PD-1/PD-L1 pathway to promote T-cell/cytokine activation may be helpful to treat cancer; however, it may accelerate the progression of atherosclerosis in patients with underlying atherosclerotic diseases.[21] The reports of thrombotic adverse events following PD-1/PD-L1 inhibitor use in clinical practice may further support this point.[22] Animal study showed that PD-L1 knockout inhibited platelet activation and thrombosis, and treatment targeting PD-L1 protected the brain against ischemic stroke.[23] Future mechanistic studies are warranted to disclose the potential mechanism relating decreased PD-L1 expression and increased vascular events.

Recently, the role of NETs in EVT-retrieved thrombi was highlighted. NETs, which were found more abundantly in more mature thrombi, were reported to form extracellular DNA networks that may stabilize the thrombus and provide resistance to fibrinolysis.[24 25] Given that NETosis has been well described to contribute to systemic inflammation and thrombogenicity in various conditions,[26–28] thrombus NET contents may reflect the propensity for recurrent thrombosis in AIS. H3Cit content of thrombus tended to correlate with CD68 (a macrophage marker), which may implicate macrophage actively interacting with NET,[29 30] subsequently leading to an increased risk of RVE.

The absence of HMGB1 positive cells in thrombus was associated with future vascular events, although its significance was lost after adjusting for clinical variables. HMGB1 bound to DNA stabilizes nucleosomes, repairs DNA, and removes damaged DNA fragments under physiological conditions.[31] HMGB1 also acts as a bone-active cytokine released by osteoblasts and osteoclasts, regulating osteogenesis, bone marrow microenvironment, and hematopoietic stem cells within the bone.[32 33] Being a reservoir of various minerals and a habitat for hematopoietic stem cells, bone has a multifaceted mechanistic link with vessels. Our previous study showed that decreased bone mineral density is associated with increased burden of cerebral small vessel disease among patients with a stroke.[34] In the present study, we found a positive correlation between the number of HMGB1-positive cells in thrombus and bone mineral density, which might suggest that weakened bone structure is associated with reduced production of cells expressing HMGB1. Nevertheless, considering the neutral association between HMGB1 expression and future vascular events after adjusting for clinical variables, future studies are required to validate the role of HMGB1-positive cells in thrombosis and atherosclerosis.

This study had several limitations. First, this study was based on a small number of patients from a single center, and thus it is currently challenging to robustly generalize our findings. Future studies with a larger sample size in multiple stroke centers are warranted for external validation. Second, this study could not include patients for whom thrombectomy failed in which thrombi were not retrieved. Factors including prior antithrombotic medication, combined thrombolytic therapy, or distal migration of the thrombus during EVT could influence complete thrombus extraction, potentially resulting in biased results. Finally, the immunologic features of thrombus were compared only among patients with AIS, as no thrombus exists in normal controls. Investigating the immunological features of thrombus from other vascular beds, such as coronary or femoral arteries, may be helpful to validate our findings.

With the extension of the EVT time window, opportunities to thoroughly examine retrieved thrombus characteristics are also increasing. This study suggests that the thrombus from EVT may provide vital information about the mechanistic clues of the index stroke, and also on the long-term clinical outcomes. Future studies are warranted to further clarify the mechanistic role of the immune signature in thrombosis and the therapeutic strategies targeting the immune signature.

Author affiliations
[1]Department of Neurology, Seoul National University Hospital, Seoul, Korea

²Department of Pathology, Chung-Ang University Hospital, Seoul, Korea
³Department of Neurology, Chung-Ang University Hospital, Seoul, Korea
⁴Department of Neurosurgery, Chung-Ang University Hospital, Seoul, Korea
⁵Department of Surgery, Chung-Ang University College of Medicine and Graduate School of Medicine, Seoul, Korea
⁶Department of Laboratory Medicine, Chung-Ang University Hospital, Seoul, Korea

ORCID iDs
Wookjin Yang http://orcid.org/0000-0001-6668-6680
Jeong-Min Kim http://orcid.org/0000-0001-7213-5527
Hae-Bong Jeong http://orcid.org/0000-0002-4937-288X
Hyun Ho Choi http://orcid.org/0000-0003-1170-6829

REFERENCES

1. Gong C, Huang J, Kong W, *et al*. Five-year outcomes after endovascular treatment for large vessel occlusion stroke. *Front Neurosci* 2022;16:920731.
2. Zhao W, Shang S, Li C, *et al*. Long-term outcomes of acute ischemic stroke patients treated with endovascular thrombectomy: a real-world experience. *J Neurol Sci* 2018;390:77–83.
3. Boeckh-Behrens T, Kleine JF, Zimmer C, *et al*. Thrombus histology suggests cardioembolic cause in cryptogenic stroke. *Stroke* 2016;47:1864–71.
4. Fitzgerald S, Dai D, Wang S, *et al*. Platelet-rich emboli in cerebral large vessel occlusion are associated with a large artery atherosclerosis source. *Stroke* 2019;50:1907–10.
5. Kim SK, Yoon W, Kim TS, *et al*. Histologic analysis of retrieved clots in acute ischemic stroke: correlation with stroke etiology and gradient-echo MRI. *AJNR Am J Neuroradiol* 2015;36:1756–62.
6. Heo JH, Nam HS, Kim YD, *et al*. Pathophysiologic and therapeutic perspectives based on thrombus histology in stroke. *J Stroke* 2020;22:64–75.
7. Kang L, Yu H, Yang X, *et al*. Neutrophil extracellular traps released by neutrophils impair revascularization and vascular remodeling after stroke. *Nat Commun* 2020;11:2488.
8. Novotny J, Oberdieck P, Titova A, *et al*. Thrombus net content is associated with clinical outcome in stroke and myocardial infarction. *Neurology* 2020;94:e2346–60.
9. Chen SH, Scott XO, Ferrer Marcelo Y, *et al*. Netosis and inflammasomes in large vessel occlusion thrombi. *Front Pharmacol* 2020;11:607287.
10. Kim SW, Lee JK. Role of HMGB1 in the interplay between netosis and thrombosis in ischemic stroke: a review. *Cells* 2020;9:1794.
11. Wang Q, Lin W, Tang X, *et al*. The roles of microRNAs in regulating the expression of PD-1/PD-L1 immune checkpoint. *Int J Mol Sci* 2017;18:2540.
12. Kim J-M, Byun J-S, Kim J, *et al*. Analysis of microRNA signatures in ischemic stroke thrombus. *J Neurointerv Surg* 2022;14:neurintsurg-2021-017597.
13. Kim J-M, Lee R, Kim Y, *et al*. Impact of metabolic activity of vertebra and amygdala on stroke recurrence: a prospective cohort study. *Circ Cardiovasc Imaging* 2023;16:e014544.
14. Lewiecki EM, Binkley N, Morgan SL, *et al*. Best practices for dual-energy X-ray absorptiometry measurement and reporting: International Society for Clinical Densitometry guidance. *J Clin Densitom* 2016;19:127–40.
15. Koh J, Kwak Y, Kim J, *et al*. High-throughput multiplex immunohistochemical imaging of the tumor and its microenvironment. *Cancer Res Treat* 2020;52:98–108.
16. Camp RL, Dolled-Filhart M, Rimm DL. X-tile: a new bio-informatics tool for biomarker assessment and outcome-based cut-point optimization. *Clin Cancer Res* 2004;10:7252–9.
17. Akinleye A, Rasool Z. Immune checkpoint inhibitors of PD-L1 as cancer therapeutics. *J Hematol Oncol* 2019;12:92.
18. Zhao S, Li F, Leak RK. Regulation of neuroinflammation through programed death-1/programed death ligand signaling in neurological disorders. *Front Cell Neurosci* 2014;8:271.
19. Bu D, Tarrio M, Maganto-Garcia E, *et al*. Impairment of the programmed cell death-1 pathway increases atherosclerotic lesion development and inflammation. *Arterioscler Thromb Vasc Biol* 2011;31:1100–7.
20. Lee J, Zhuang Y, Wei X, *et al*. Contributions of PD-1/PD-L1 pathway to interactions of myeloid DCs with T cells in atherosclerosis. *J Mol Cell Cardiol* 2009;46:169–76.
21. Foks AC, Kuiper J. Immune checkpoint proteins: exploring their therapeutic potential to regulate atherosclerosis. *Br J Pharmacol* 2017;174:3940–55.
22. Kunimasa K, Nishino K, Kimura M, *et al*. Pembrolizumab-induced acute thrombosis. *Medicine* 2018;97:e10772.
23. Li Y, Xin G, Li S, *et al*. PD-L1 regulates platelet activation and thrombosis via caspase-3/GSDME pathway. *Front Pharmacol* 2022;13:921414.
24. Laridan E, Denorme F, Desender L, *et al*. Neutrophil extracellular traps in ischemic stroke thrombi. *Ann Neurol* 2017;82:223–32.
25. Ducroux C, Di Meglio L, Loyau S, *et al*. Thrombus neutrophil extracellular traps content impair tPA-induced thrombolysis in acute ischemic stroke. *Stroke* 2018;49:754–7.
26. Delgado-Rizo V, Martínez-Guzmán MA, Iñiguez-Gutierrez L, *et al*. Neutrophil extracellular traps and its implications in inflammation: an overview. *Front Immunol* 2017;8:81.
27. Demers M, Wagner DD. NETosis: a new factor in tumor progression and cancer-associated thrombosis. *Semin Thromb Hemost* 2014;40:277–83.
28. Mozzini C, Garbin U, Fratta Pasini AM, *et al*. An exploratory look at netosis in atherosclerosis. *Intern Emerg Med* 2017;12:13–22.
29. Monteith AJ, Miller JM, Maxwell CN, *et al*. Neutrophil extracellular traps enhance macrophage killing of bacterial pathogens. *Sci Adv* 2021;7:eabj2101.
30. Nakazawa D, Shida H, Kusunoki Y, *et al*. The responses of macrophages in interaction with neutrophils that undergo netosis. *J Autoimmun* 2016;67:19–28.
31. Ye Y, Zeng Z, Jin T, *et al*. The role of high mobility group box 1 in ischemic stroke. *Front Cell Neurosci* 2019;13:127.
32. Yang J, Shah R, Robling AG, *et al*. HMGB1 is a bone-active cytokine. *J Cell Physiol* 2008;214:730–9.
33. Yuan S, Liu Z, Xu Z, *et al*. High mobility group box 1 (HMGB1): a pivotal regulator of hematopoietic malignancies. *J Hematol Oncol* 2020;13:91.
34. Kim J-M, Park K-Y, Kim HR, *et al*. Association of bone mineral density to cerebral small vessel disease burden. *Neurology* 2021;96:e1290–300.